

Global optimization of additive potential energy functions: Predicting binary Lennard-Jones clusters

István Kolossváry^{1,2,*} and Kevin J. Bowers³¹*Department of Chemistry, Budapest University of Technology and Economics, H-1111 Budapest, Hungary*²*BIOKOL Research, LLC, Madison, New Jersey 07940, USA*³*Los Alamos National Laboratory, Los Alamos, New Mexico 87545, USA*

(Received 9 September 2010; revised manuscript received 13 October 2010; published 18 November 2010)

We present a method for minimizing additive potential-energy functions. Our *hidden-force algorithm* can be described as an intricate multiplayer tug-of-war game in which teams try to break an impasse by randomly assigning some players to drop their ropes while the others are still tugging until a partial impasse is reached, then, instructing the dropouts to resume tugging, for all teams to come to a new overall impasse. Utilizing our algorithm in a non-Markovian parallel Monte Carlo search, we found 17 new putative global minima for binary Lennard-Jones clusters in the size range of 90–100 particles. The method is efficient enough that an unbiased search was possible; no potential-energy surface symmetries were exploited. All new minima are comprised of three nested polyicosahedral or polytetrahedral shells when viewed as a nested set of Connolly surfaces (though the shell structure has previously gone unscrutinized, known minima are often qualitatively similar). Unlike known minima, in which the outer and inner shells are comprised of the larger and smaller atoms, respectively, in 13 of the new minima, the atoms are not as clearly separated by size. Furthermore, while some known minima have inner shells stabilized by larger atoms, four of the new minima have outer shells stabilized by smaller atoms.

DOI: [10.1103/PhysRevE.82.056711](https://doi.org/10.1103/PhysRevE.82.056711)

PACS number(s): 05.10.–a, 61.46.Bc, 36.40.Mr

I. INTRODUCTION

Binary Lennard-Jones (BLJ) clusters can only be considered as a crude representation of practical nanoalloys (mostly metallic with many-body interactions) [1–3]; nevertheless, they provide a good starting point for studying these materials and are theoretically particularly interesting for the momentous difficulty required to search their intricate multidimensional configuration space [4,5]. A BLJ cluster consists of a fixed number of atoms. There are only two atom types and they differ in size and, in general, in their cohesive energies; however, in what follows only the size differs for fair comparison with prior work in this field [4,5]. Minimizing a BLJ cluster requires searching an exceedingly rugged continuous potential-energy surface for each discrete cluster composition. Cluster minimization methods can be split into two categories: biased and unbiased [6]. Biased methods were first used for clusters of a single atom type and conduct a restricted search within an immensely reduced configuration space of some configuration symmetry group assumed *a priori* (or in some cases start with an educated guess based on intuition or prior knowledge); unfortunately, BLJ clusters often lack the symmetries required to make biased methods effective. Unbiased methods start with a random configuration and gradually lower the energy by iterative application of geometric perturbations and local minimization, usually with a Monte Carlo scheme. BLJ cluster minimization method of Doye and Meyer [4,5] is based on the very successful basin-hopping method developed by Wales and Doye [7–9] which, in turn, is based on the Monte Carlo minimiza-

tion method of Li and Scheraga [10]. The method of Doye and Meyer uses the basin-hopping move set of Wales and Doye (random atomic displacements and rotation of low-energy atoms around the center of mass) augmented with swapping two randomly selected atoms' types and changing a single randomly selected atom's type for numerous Monte Carlo searches. Each Monte Carlo search has a fixed temperature and is periodically restarted using low-energy intermediate configurations discovered by previous searches [5,11]. Our approach is built on a novel move set which we call the *hidden-force algorithm* (HFA). We embed this move set in a scheme that generalizes the Monte Carlo search of Doye and Meyer to exploit parallel computation effectively.

II. HIDDEN-FORCE MONTE CARLO ALGORITHM

HFA exploits that, for an additive potential, the potential-energy gradient is also additive. At local minima, the gradient vanishes $\partial V / \partial x_i = 0, \forall i$, where x_i is the position of atom i along axis x (and similarly for the y and z axes). Concentrating on pairwise additive potentials, we have $\partial V / \partial x_i = \sum_j \partial V_{ij} / \partial x_i$, where V_{ij} is the interaction energy between atoms i and j . Though the gradient components sum to zero at local minima, each term's magnitude is generally nonzero. Like a multiteam tug of war at an impasse, significant opposing forces (the negative of the gradient) may be exerted upon cluster atoms. Disrupting this network of opposing forces will result in the collective rearrangement of cluster atoms. Using the tug-of-war analogy to describe the basic HFA move, one such disruption is for some teams (atoms) to drop simultaneously their ropes (drop their interactions from the potential-energy function). The remaining teams then rearrange due to their net nonzero tugging and reach a partial impasse. At this point, the dropouts resume tugging until a

*Present address: D. E. Shaw Research, LLC, New York, NY 10036, USA; istvan@kolossvary.hu

new overall impasse is achieved. Specifically, given a local minimum-energy configuration, all of the interactions of a randomly selected subset of the cluster atoms are temporarily dropped and the configuration of the remaining atoms is locally minimized. The original potential-energy function is then used to reminimize the entire cluster. Because the dropped atoms remain at their original positions, they may be brought in close proximity with the remaining atoms. Much like the tug-of-war players cannot occupy the same position on the playing field (whether or not they are tugging), we do not allow dropped atoms to come into close proximity with other atoms via a simple iterative procedure. This avoids huge repulsive forces that can adversely affect the final minimization. There is no guarantee that the resulting cluster configuration will be lower in energy than the starting configuration, but we have found HFA to be an exceptionally successful move set in a Monte Carlo cluster minimization. Significantly, the HFA trial configuration is highly dependent on the starting configuration since the move is driven by forces already present. Accordingly, the HFA Monte Carlo search will be non-Markovian and has a slight hint of a partially genetic algorithm (with no crossover) in that low-energy clusters tend to represent tug-of-war impasse configurations where the internal forces are “advantageous” with respect to the survival, i.e., the gradual lowering of the energy of new generations of configurations as the search progresses.

The HFA Monte Carlo search strategy is outlined as follows.

Initialize search with a random configuration (and, if applicable, with a random composition) and minimize it. Add the structure to a set of low-energy configurations called the restart pool.

Main iteration loop:

(1) If a binary cluster search (with two atom types) and a long stretch of the hidden-force Monte Carlo algorithm (HFA-MC) iterations [(2)–(7) below] with the current composition have not produced a new global minimum configuration, apply single or multiple mutations by flipping the atom type of randomly selected atoms.

(2) Apply an HFA move.

(3) Accept the trial configuration if the trial energy is less than the minimum of the current configuration energy plus some user-defined energy window and the best minimum energy seen plus some other user-defined energy window. The second energy window is necessary to prevent accepting a long succession of small uphill energy movements. If rejected, revert to current configuration or composition and go to (6).

(4) Make the trial configuration and composition the current configuration and check if it is structurally unique to eliminate duplicates. Uniqueness is tested with a simple hash function including the energy, composition, and cluster radius of gyration. If a unique structure, add to the restart pool.

(5) If the current configuration is the best minimum seen, remove restart pool configurations that are outside the new best minimum-energy window. (Note that the restart pool typically includes low-energy configurations with different compositions.)

(6) If, after a user-defined number of iterations, there have been no improvements to the best minimum seen, set the

current configuration to one selected from the restart pool at random and go to (1) (Since this HFA Monte Carlo algorithm is non-Markovian, the search can get stuck in a limited volume of configuration space from the HFA interdependence of successive configurations along the search path. We found the periodic restarts very effective in dealing with this problem.)

(7) If running in parallel and a user-defined number of iterations have elapsed, copy the restart pool from the search with the overall best minimum seen to the local restart pool, set the current configuration to one selected from the restart pool at random, and go to (1) (The HFA Monte Carlo search method is most efficient when using numerous searches run in parallel seeded with different starting configurations. We found that a simple winner-takes-all strategy applied to a set of linked searches can often find the global minimum faster than an equal number of independent searches.)

(8) If after a user-defined number of iterations the overall best minimum seen energy has not improved to a user-defined energy, return the best minimum energy seen. (We also found that ill-fated searches were likely to get stuck sooner than later and, therefore, searches not showing sufficient progress will be aborted to free up computational resources for new searches started from scratch.)

III. RESULTS AND DISCUSSION

Search particulars are as follows. The potential is the standard BLJ potential, $V_{BLJ} = 4\sum_{i<j}\epsilon_{AB}[(\sigma_{AB}/r_{ij})^{12} - (\sigma_{AB}/r_{ij})^6]$, where A and B are the atom types, i and j are atom indices, $\epsilon_{AB} \equiv 1$ is the uniform well depth, $\sigma_{AB} = (\sigma_{AA} + \sigma_{BB})/2$ and multiplied by $2^{1/6}$ gives the equilibrium pair separation between atoms i and j (with $\sigma_{AA} \equiv 1$ set to be the unit of length), and r_{ij} is the distance. The size ratio of atom types A and B is $\sigma_{AA}/\sigma_{BB} \leq 1$, with A always referring to the smaller atom. The HFA move in (2) above involved 10–25 % of the cluster atoms. The energy windows in (3) were set to $0.15\epsilon_{AB}$ and $0.25\epsilon_{AB}$, respectively, and the latter window was also used for updating the restart pool in (5). Searches were initiated with an approximately half-and-half A/B composition and run for 1×10^6 iterations unless aborted in (8), which took approximately six CPU hours each for clusters in the size range of 90–100 particles on a standard 2.4 GHz Intel processor utilizing single instruction, multiple data (SIMD) vector acceleration in all force computations and linear algebra operations. The iteration intervals referred to in (1), (6), and (7) were set, respectively, to 10 000, 1000, and 100 000. We wrote a customized version of the limited-memory Broyden-Fletcher-Goldfarb-Shanno (LBFGS) preconditioned truncated Newton conjugate gradient method for local minimizations [12] utilizing analytical second derivatives in a sparse Hessian representation. In our preliminary tests we reproduced all global minima previously found for LJ clusters of up to 150 particles [13], including the hard to find tetrahedral global minimum of LJ₉₈ [14], and also successfully located the putative global minima of the much larger LJ₃₄₂ and LJ₃₄₇ clusters [15]. The focus of our present work was revisiting the largest BLJ clusters reported in the Cambridge Cluster Database (CCDB) [16] in the size range of 90–100 particles [17,18].

TABLE I. Energies of the 17 new putative global minima listed in ε units, relative to the previous best energies in the CCDB [17]. The numbers in parentheses in the “Energy” columns show the number of additional unique clusters found with the same number of particles (but in most cases with different A/B compositions) that had energies still lower than the base energy. The “Cluster” columns identify the clusters and the “No.” columns list the labels used in the text. Clusters 4 and 11 shown in bold have lower energies than those reported in [11] and their structures are also significantly different (see text). The coordinates of the new putative global minima have been deposited in the CCDB [23].

No.	Cluster	Energy, [ε]	No.	Cluster	Energy, [ε]
1	BLJ ₉₂ , $N_A=28$, $\sigma_{BB}=1.15$	-0.014670 (0)	10	BLJ ₉₇ , $N_A=41$, $\sigma_{BB}=1.30$	-1.500728 (3)
2	BLJ ₉₃ , $N_A=31$, $\sigma_{BB}=1.15$	-0.156480 (0)	11	BLJ₉₈, $N_A=39$, $\sigma_{BB}=1.25$	-0.295878 (1)
3	BLJ ₉₄ , $N_A=31$, $\sigma_{BB}=1.15$	-0.766377 (3)	12	BLJ ₉₈ , $N_A=41$, $\sigma_{BB}=1.30$	-1.428041 (4)
4	BLJ₉₅, $N_A=34$, $\sigma_{BB}=1.20$	-0.440722 (1)	13	BLJ ₉₉ , $N_A=42$, $\sigma_{BB}=1.25$	-1.082912 (7)
5	BLJ ₉₆ , $N_A=33$, $\sigma_{BB}=1.20$	-0.957821 (4)	14	BLJ ₉₉ , $N_A=42$, $\sigma_{BB}=1.30$	-1.248290 (2)
6	BLJ ₉₆ , $N_A=39$, $\sigma_{BB}=1.25$	-0.203123 (0)	15	BLJ ₁₀₀ , $N_A=35$, $\sigma_{BB}=1.20$	-0.024301 (0)
7	BLJ ₉₆ , $N_A=41$, $\sigma_{BB}=1.30$	-0.606835 (1)	16	BLJ ₁₀₀ , $N_A=42$, $\sigma_{BB}=1.25$	-1.202295 (7)
8	BLJ ₉₇ , $N_A=33$, $\sigma_{BB}=1.20$	-0.495369 (0)	17	BLJ ₁₀₀ , $N_A=42$, $\sigma_{BB}=1.30$	-1.424056 (3)
9	BLJ ₉₇ , $N_A=39$, $\sigma_{BB}=1.25$	-0.252938 (0)			

We conducted a total of 66 searches on BLJ₉₀ to BLJ₁₀₀ varying the size of the type B atoms σ_{BB} between 1.05 and 1.3 keeping $\sigma_{AA}=1$. The energies of the 17 new putative global minima are listed in Table I in ε units, relative to the previous best energies in the CCDB [17] (as of July 2010). The remaining 49 searches furnished the same global minima already found. (An additional 36 unique clusters were found during these searches that had energies lower than these known minima, in most cases with different A/B compositions.) We then used the Maestro molecular modeling environment [19] to analyze the structures as a set of nested shells. We first constructed the convex hull of the entire cluster using the Connolly surface [20] with a $2.5\sigma_{AA}$ probe radius [21]. At this probe radius, atoms on the Connolly surface empirically either occupied a vertex on the convex hull or were positioned just within the convex hull. We removed these atoms and repeated the above until no atoms remained. The first set of atoms removed constituted the outer shell, the second set constituted the middle shell, and so forth.

We found that all 17 new global minima were made of three shells. In some cases the shells were homogenous with the outer shell exclusively made of the larger (type B) atoms and the inner shells made of smaller (type A) atoms (clusters 13, 14, 16, and 17, all with C_S symmetry belong to this class). Figure 1 shows such a separation: Fig. 1(a) shows the nested shells and Figs. 1(b)–1(d), respectively, the outer, middle, or inner shells (type A in dark gray/maroon and type B in light gray/green). The cluster shown in Fig. 1 is the putative global minimum of BLJ₉₈/ $\sigma_{BB}=1.25$ reported in [11] with $E=-584.930661$ in ε units and C_S symmetry, comprised of 42 type A atoms packed inside the shell of 56 type B atoms. Cluster 11 found by our HFA search shown in Fig. 2 has, in fact, slightly lower energy (-584.953979ε) and only 39 type A atoms, but more importantly the new putative global minimum configuration of BLJ₉₈/ $\sigma_{BB}=1.25$ has an entirely different structure with no symmetry. Our unexpected finding demonstrates that, unlike previous BLJ

minima in this size range, this cluster has a type A atom in the outer shell [22]. Figure 2(b) shows a single type A atom (dark gray/maroon) touching the surface of the outer shell, but not lodged in a vertex position, and Fig. 2(c) shows two explicitly plotted B type atoms (light gray/green) in the middle shell; one surfacing in a similar fashion and the other occupying a lattice point. Figure 2(d) displays an additional type B atom occupying a vertex of the inner shell.

Similar to cluster 11 every other new minimum with the exception of the aforementioned pure-shell clusters has a few

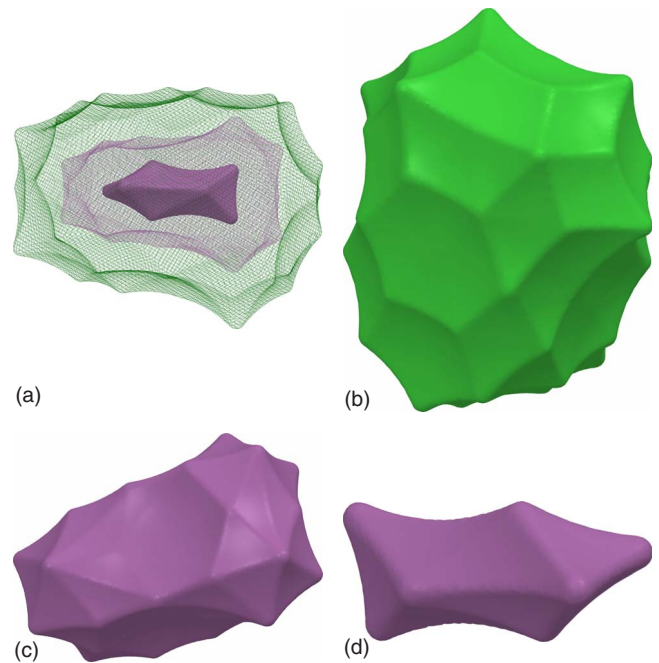


FIG. 1. (Color online) Cluster BLJ₉₈/ $\sigma_{BB}=1.25$ [11] shown in the nested convex hull representation: (a) nested shells, (b) outer shell, (c) middle shell, and (d) inner shell. Type A atoms in dark gray/maroon; type B atoms in light gray/green. Atoms are located at vertices; they are not shown explicitly.

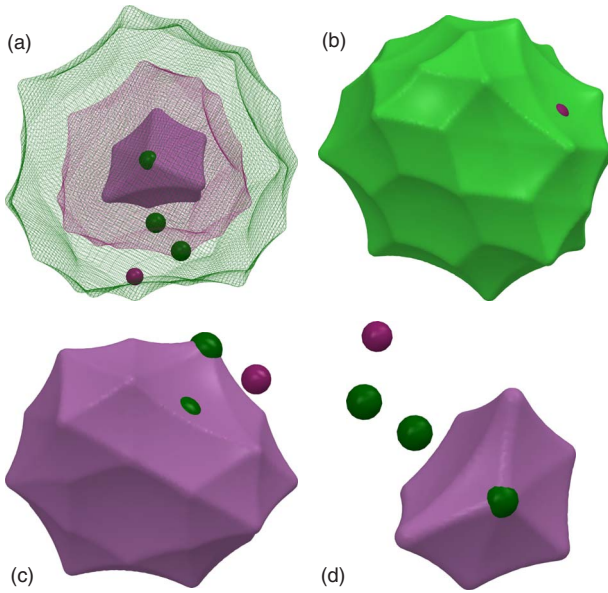


FIG. 2. (Color online) Our new putative global minimum configuration of cluster $BLJ_{98}/\sigma_{BB}=1.25$ (cluster 11) shown in the nested convex hull representation: (a) nested shells, (b) outer shell, (c) middle shell, and (d) inner shell. Atoms not positioned at lattice points of their own type are displayed explicitly (type A dark gray/maroon; type B light gray/green) (see text for details).

cuckoo’s egg atoms alloyed with the dominant atom type of some or all of the three shells. In clusters 1–3, 5, 7, 8, 10, 12, and 15, the B atoms inside the outer shell occupy convex hull vertices of a mixed type middle and/or inner cage. In addition to such B atoms, clusters 4 and 11 have a single A atom and clusters 6 and 9 have two A atoms lodged in the outer shell. The minimum-energy configuration of cluster $BLJ_{95}/\sigma_{BB}=1.2$ (with 33 type A atoms and $E=-557.690\,639\epsilon$) [11] shown in Fig. 3 exemplifies a pure B type outer shell and mixed type middle and inner shells occupying vertices in predominantly A type shells. Type B atoms lodged at type A lattice vertices are displayed explicitly (type B light gray/green; type A dark gray/maroon). Our new putative global minimum in Fig. 4 has slightly lower energy ($-557.785\,217\epsilon$) and its structure is virtually identical to that of Fig. 3 with one additional type A atom, which appears in the middle of a pentagonal pane in the outer convex hull. Figures 3 and 4 are oriented the same way to highlight the difference in local structure around the type A atom in the outer shell [cf. Figs. 3(b) and 4(b)]. Type B atoms inside the outer shell have been previously found in some polytetrahedral clusters and were characterized in the framework of the so-called “disclination” network [4,5]. Our nested shell view reveals that these B atoms are integral to a predominantly A type cage structure. We further conclude that there are two types of “impurities” in BLJ clusters: a common case where a type B atom substitutes for a type A atom vertex in an inner shell (and potentially vice versa though we have not yet found an example) and an exceptional case in which either atom type appears as a “pockmark” on the shell surface.

Besides structural features of the new minima we also looked at overall cluster stability in this size range. Following the analysis of Doye and Meyer [4,5] we were looking

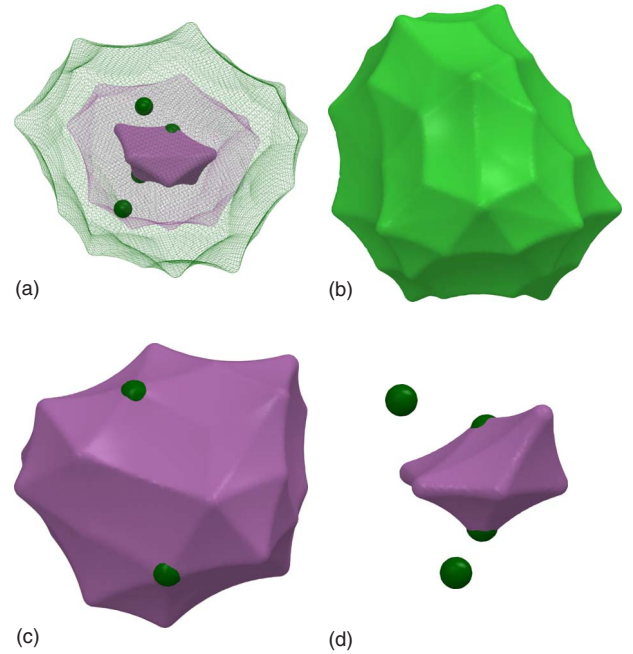


FIG. 3. (Color online) Cluster $BLJ_{95}/\sigma_{BB}=1.2$ [11] shown in the nested convex hull representation: (a) nested shells, (b) outer shell, (c) middle shell, and (d) inner shell. Type B atoms (light gray/green) lodged at type A lattice vertices (dark gray/maroon) are displayed explicitly.

for “magic numbers” in terms of particularly stable cluster sizes for a given B/A particle size ratio. Figure 5 shows six stability curves of the six size ratios that were considered in this work. Cluster stability is measured by $E_{\text{glb}}(N)-E_{\text{fit}}(N)$ in ϵ units as a function of cluster size N . E_{glb} is the global minimum energy found for a particular cluster size with a fixed size ratio and E_{fit} is the fitted energy value of the function $a+bN^{1/3}+cN^{2/3}+dN$, where the parameters a , b , c , and d were obtained by least-squares fit to the same E_{glb} values [5]. Local minima on the stability curves represent magic numbers corresponding to cluster sizes that give rise to structures with extra stability relative to neighboring sizes. Magic numbers are particularly sensitive to the size ratio. Figure 5 clearly identifies BLJ_{95} as magic number cluster for size ratios of 1.05 and 1.1, BLJ_{94} at 1.15, and BLJ_{93} and BLJ_{97} at 1.3, whereas it is not clear whether size ratios 1.2 and 1.25 provide genuine magic numbers even though both have multiple local minima on their respective stability curves.

IV. SUMMARY

In this paper we present our HFA-MC for global optimization of additive objective functions. HFA is based on the simple idea of a multiplayer tug-of-war game where teams interact by tugging on their ropes. The teams can represent physical particles such as Lennard-Jones particles in our case study interacting via a simple LJ potential or any other types of particles including ions and molecules forming nanoclusters. Moreover, the teams can also represent entities from other disciplines such as social sciences or economics when an optimal solution is sought in an abstract configuration

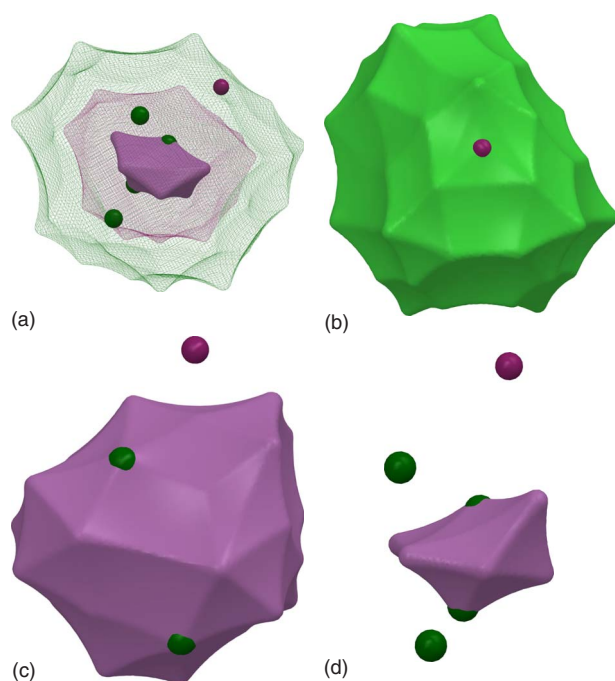


FIG. 4. (Color online) Our new putative global minimum configuration of cluster $BLJ_{95}/\sigma_{BB}=1.2$ (cluster 4) shown in the nested convex hull representation: (a) nested shells, (b) outer shell, (c) middle shell, and (d) inner shell. Atoms not positioned at lattice points of their own type are displayed explicitly (type A dark gray/maroon; type B light gray/green) (see text for details).

space of interacting people or groups of people or some economic units such as interacting banks or companies (provided that an appropriate model interaction-potential function is defined). Our study on binary Lennard-Jones clusters

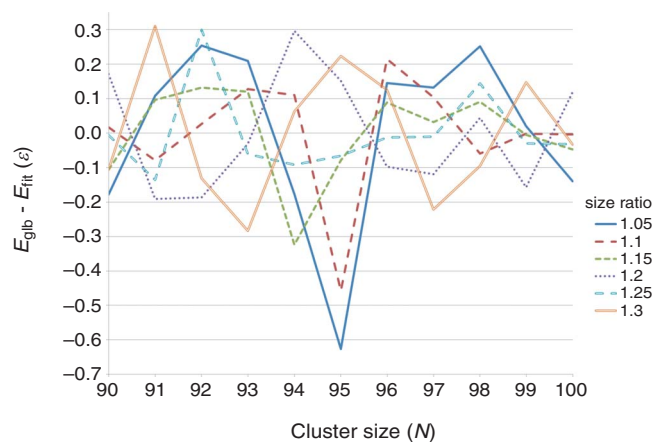


FIG. 5. (Color online) Cluster stability measured by $E_{\text{glb}}(N) - E_{\text{fit}}(N)$ in ϵ units as a function of cluster size N . E_{glb} is the global minimum energy found for a particular cluster size with a fixed B/A size ratio and E_{fit} is the fitted energy value of the function $a + bN^{1/3} + cN^{2/3} + dN$, where the parameters a , b , c , and d were obtained by least-squares fit to the same E_{glb} values [5]. Local minima on the stability curves correspond to magic numbers explained in the text.

has not only found numerous new putative global minima, but utilizing our visual inspection method of convex hulls has revealed that while some known minima have inner shells stabilized by larger atoms, four of the new minima have outer shells stabilized by smaller atoms (at the occasional expense of breaking symmetry). We also identified a few particularly stable, so-called, magic number clusters. Our current research is aimed at clusters subject to implicit geometric constraints arising from multibody potentials.

- [1] J. A. Alonso, *Structure and Properties of Atomic Nanoclusters* (Imperial College Press, London, 2005), pp. 205–227.
- [2] S. Neukermans, E. Janssens, R. E. Silverans, and P. Lievens, in *Atomic Clusters: From Gas Phase to Deposited*, edited by D. P. Woodruff (Elsevier, Oxford, UK, 2007), pp. 271–297.
- [3] G. M. Pastor and J. Dorantes-Dávila, in *Atomic Clusters: From Gas Phase to Deposited*, edited by D. P. Woodruff (Elsevier, Oxford, UK, 2007), pp. 550–554.
- [4] J. P. K. Doye and L. Meyer, *Phys. Rev. Lett.* **95**, 063401 (2005).
- [5] J. P. K. Doye and L. Meyer, e-print [arXiv:cond-mat/0604250](https://arxiv.org/abs/cond-mat/0604250).
- [6] X. Shao, X. Yang, and W. Cai, *J. Comput. Chem.* **29**, 1772 (2008).
- [7] D. J. Wales and J. P. K. Doye, *J. Phys. Chem. A* **101**, 5111 (1997).
- [8] J. P. K. Doye and D. J. Wales, *Phys. Rev. Lett.* **80**, 1357 (1998).
- [9] J. P. K. Doye, D. J. Wales, and M. A. Miller, *J. Chem. Phys.* **109**, 8143 (1998).
- [10] Z. Li and H. A. Scheraga, *Proc. Natl. Acad. Sci. U.S.A.* **84**, 6611 (1987).
- [11] Recently, we learned about a preprint in which the basin-hopping method was successfully utilized with molecular dynamics based moves. M. Sicher, S. Mohr, and S. Goedecker, e-print [arXiv:1006.5675](https://arxiv.org/abs/1006.5675).
- [12] J. Nocedal and J. L. Morales, *SIAM J. Optim.* **10**, 1079 (2000).
- [13] <http://physchem.ox.ac.uk/~doye/jon/structures/LJ/tables.150.html>
- [14] R. H. Leary and J. P. K. Doye, *Phys. Rev. E* **60**, R6320 (1999).
- [15] Y. Xiang, H. Jiang, W. Cai, and X. Shao, *J. Phys. Chem. A* **108**, 3586 (2004).
- [16] D. J. Wales, J. P. K. Doye, A. Dullweber, M. P. Hodges, F. Y. Naumkin, F. Calvo, J. Hernández-Rojas, and T. F. Middleton, <http://www-wales.ch.cam.ac.uk/CCD.html>.
- [17] <http://physchem.ox.ac.uk/~doye/jon/structures/BLJ/table.html>.
- [18] 15 out of our 17 new minima were independently found by Sicher, Mohr, and Goedecker using a significantly different search method [11], http://www-wales.ch.cam.ac.uk/~wales/CCD/NEW_BINARY_LJ_MINIMA/
- [19] <http://www.schrodinger.com/products/14/12/>
- [20] M. L. Connolly, *J. Appl. Crystallogr.* **16**, 548 (1983).

- [21] We found the $2.5\sigma_{AA}$ probe radius empirically. A radius much smaller than the equilibrium particle separation fails to form a shell. A radius much larger asymptotically becomes the convex hull. We found the intermediate value helpful to identify both atoms on the convex hull and atoms interior to but near the convex hull.
- [22] The presence of type A atom(s) in the outer shell has been overlooked. For example, the previous best $BLJ_{99}/\sigma_{BB}=1.25$ minimum seen in the CCDB [17] also features a single type A atom in the outer shell.
- [23] http://www-wales.ch.cam.ac.uk/~wales/CCD/Istvan_kolossvary_new_BLJ_minima.tgz/